

# Multilayer Inkjet Printing of Millimeter-Wave Proximity-Fed Patch Arrays on Flexible Substrates

Benjamin S. Cook, *Student Member, IEEE*, Bijan Tehrani, *Student Member, IEEE*,  
James R. Cooper, *Student Member, IEEE*, and Manos M. Tentzeris, *Fellow, IEEE*

**Abstract**—Flexible inkjet-printed proximity-fed patch antennas, designed for the 24-GHz Industrial, Scientific, and Medical (ISM) band, are demonstrated in this letter for the first time featuring a multilayer inkjet deposition process. Inkjet printing of antennas allows for the low-cost, noncontact, and additive fabrication of RF components onto nearly any host substrate or package. The inkjet-printing process exhibited in this letter is the first inkjet process to demonstrate multilayer printed antennas, enabled by a new printable dielectric ink that allows for the deposition of thick dielectric layers. Printed coupled patch antennas with realized gains of over 4 dBi and four-element coupled patch arrays with gains of over 7 dBi are demonstrated on a flexible liquid crystal polymer (LCP) substrate. The antenna gain, return loss, and pattern are presented and demonstrate the repeatability and design flexibility of the novel inkjet-deposition process.

**Index Terms**—Flexible substrates, inkjet printing, inkjet-printed antennas, millimeter-wave, multilayer antenna.

## I. INTRODUCTION

INKJET printing is a fabrication technology that has attracted significant attention over the last decade as a method to rapidly fabricate low-cost passive and active devices including lumped components, low-frequency planar antennas, diodes, and thin-film transistors. Printing has the advantage of being able to deposit a wide variety of materials including conductors, dielectrics, and active materials, such as carbon nanotubes and semiconducting polymers [1]–[5]. The additive and noncontact nature of the process makes it very conducive to fabricating electronics on a wide variety of substrates ranging from flexible and organic substrates, such as paper and plastic, to more conventional substrates, such as silicon and glass wafers.

Historically, inkjet printing has been used in the RF field to fabricate low-frequency, single-layer passive components and antennas for RFID applications [6]. However, recent advances have demonstrated the printing of multilayer structures for RF applications in the low-gigahertz range such as parallel-plate capacitors [2]. By extending on these recent advances, inkjet technology can be utilized to fabricate multilayer millimeter-wave (mm-wave) components and antennas

directly onto conformal substrates, wafers, and integrated circuit (IC) packaging to increase the level of integration available to the growing mm-wave wireless industry. Conventionally, mm-wave antennas have been fabricated on multilayer laminate circuit boards or wafers that are patterned using subtractive fabrication techniques. Subtractive processes are costly and time-consuming and produce large amounts of material and chemical waste [7]–[9]. However, by enabling the direct and rapid printing of mm-wave antennas onto ICs and packages, a new level of flexible design capabilities that are not available with traditional RF fabrication techniques becomes available.

In this letter, a new multilayer, substrate-independent inkjet process is presented that can deposit highly conductive metal layers and, for the first time, incorporates the printing of thick polymer dielectric layers to replace multilayer laminates needed for RF component fabrication. The process, tuned for the Dimatix printing platform, is utilized to demonstrate multilayer proximity-coupled patch antennas and antenna arrays for the 24-GHz Industrial, Scientific, and Medical (ISM) band. The return loss and radiation pattern of the antennas are characterized, and a comparison of the repeatability between fabrication runs is presented. The results demonstrate the current ability to rapidly and reliably fabricate multilayer mm-wave antennas utilizing a low-cost inkjet printing platform.

## II. MULTILAYER INKJET FABRICATION PROCESS

The multilayer inkjet process designed for RF components is optimized for the Dimatix-2831 printing platform. The Dimatix platform is a piezo drop-on-demand printing platform that can produce feature sizes down to 20  $\mu\text{m}$  and layer registration within 5  $\mu\text{m}$  [1].

To pattern the metal layers, Cabot CCI-300 silver nanoparticle ink (Cabot Corporation, Boston, MA, USA), which is composed of 20 w% silver nanoparticles suspended in an alcohol solution, is used as received with a viscosity of 12 cP and surface tension of 30 dyn/cm. Upon printing, the silver nanoparticle ink is sintered in an oven at 180 °C for 10 min. A single printed pass at 20  $\mu\text{m}$  drop spacing yields layer thicknesses of 500 nm with a conductivity of 1.1e7 S/m [1].

To pattern the dielectric layers, a new long-chain polymer ink is formulated to produce dielectric layers with thicknesses up to 100  $\mu\text{m}$ , and above, while also having a surface chemistry compatible with that of the printed silver ink. Being able to pattern thick dielectric layers is the enabling factor in printing multilayer RF components, as previous printed dielectrics were only able to produce thicknesses on the order of 0.1–1  $\mu\text{m}$  [3], [10]. The polymer ink is formulated by loading 35 w% of an SU-8 polymer (MicroChem, Newton, MA, USA) in cyclopentanone

Manuscript received August 13, 2013; accepted September 19, 2013. Date of publication October 16, 2013; date of current version October 23, 2013. This work was supported by the NSF under a grant and the NEDO under a grant.

The authors are with the School of Electrical and Computer Engineering, Georgia Institute of Technology, Atlanta, GA 30332 USA (e-mail: benjamin.cook@gatech.edu).

Color versions of one or more of the figures in this letter are available online at <http://ieeexplore.ieee.org>.

Digital Object Identifier 10.1109/LAWP.2013.2286003

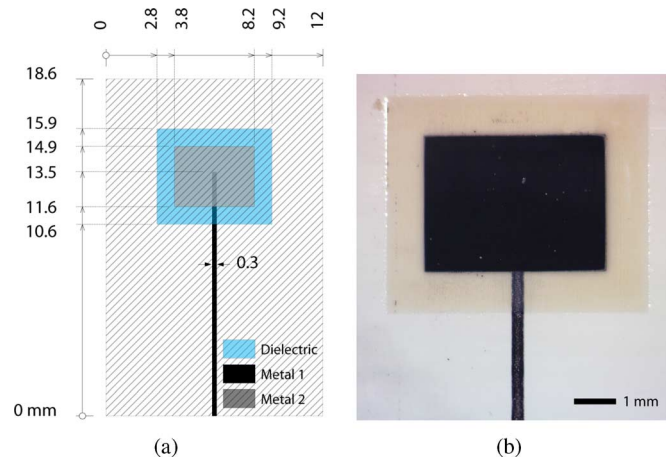


Fig. 1. (a) Design of the multilayer coupled patch antenna. (b) Optical micrograph of the fabricated coupled patch antenna on LCP substrate.

along with a UV-cross-linking agent to obtain a solution with a viscosity of 13.4 cP and a surface tension of 30 dyn/cm. Upon printing, the SU-8 ink is exposed to 150 mJ/cm<sup>2</sup> of 365 nm UV light, and then heated to 120 °C for 5 min. A single printed pass at 20 μm drop spacing yields layer thickness of 12–15 μm, which is on the order of variation of commercial laminates [11]. The permittivity ( $\epsilon_r$ ) of the SU-8 polymer is approximately 2.7, and the loss tangent ( $\tan \delta$ ) is 0.04 at 24.5 GHz [12].

The host substrate is 100 μm single-clad liquid crystal polymer (LCP) (Rogers Corporation, Rogers, CT, USA) with a permittivity of 2.9 and a loss tangent of 0.003 [11].

### III. PROXIMITY-FED PATCH DESIGN AND MEASUREMENTS

To demonstrate the advantages of the multilayer inkjet process for package-integrated mm-wave antennas, a proximity-coupled patch antenna is designed for the 24.5-GHz ISM band. Proximity-coupled patch antennas have the advantage of featuring a wider bandwidth and are easier to tune than standard microstrip or probe-fed patch antennas. However, this comes at the cost of requiring multilayer boards [13], [14]. The proposed proximity coupled patch is shown in Fig. 1(a). Utilizing the physical and electrical parameters of the characterized printing process from Section II, the CST frequency domain solver is used to optimize the antenna to have an input impedance of 50 Ω at 24.5 GHz while maximizing realized gain in the broadside direction.

To determine the required thickness of the silver layers, the skin depth is calculated to be approximately 1 μm at the center frequency of operation. Two batches of the antennas have been printed with three layers of silver (1.5 μm thickness), and five layers of silver (2.5 μm thickness), to verify that the skin depth requirements are met with three or more layers of silver. The SU-8 thickness is chosen to be 40 μm or three printed layers of SU-8 to set the correct coupling between the feed and patch for 50-Ω matching. The optimized coupled patch antennas are fabricated utilizing the layer-by-layer inkjet deposition process shown in Fig. 2. First, three layers of silver nanoparticle ink are deposited and heat-cured to form the microstrip feedline and alignment marks for layer registration. Three layers of the SU-8 dielectric are then deposited and UV-cured to form the dielectric

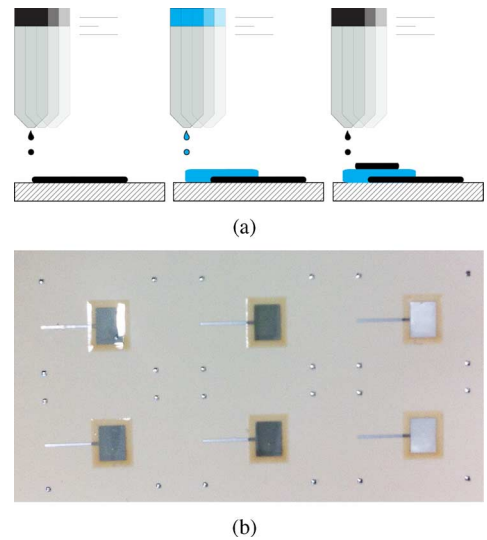


Fig. 2. (a) Process of fabricating multilayer printed patch antennas. (b) Final fabricated batch of printed patch antennas.

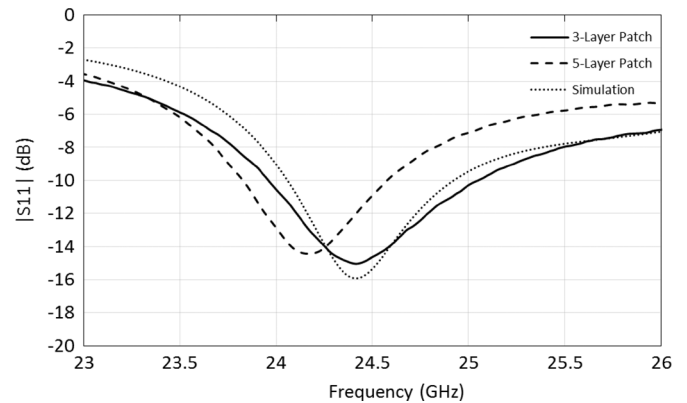


Fig. 3. Simulated and measured return loss of the coupled patch antenna.

spacer. A final three layers of silver are deposited and heat-cured to pattern the microstrip patch. The same process is repeated for the patch antennas utilizing five layers of silver.

An optical micrograph of the fabricated patch antenna prototype is shown in Fig. 1(b). Post-fabrication measurements show the dielectric thickness to be 35 μm, and the patch length and width to be 3.38 and 4.52 mm, respectively. The slightly longer length and width dimensions of the patch from the layout are caused by drop spreading as the printing software specifies drops centered on the borders of the layout. The slight changes in dimensions are accounted for in the final simulations. Following fabrication, the LCP carrier substrate is diced, and clamp-mount Southwest Microwave end-launch connectors are affixed to the antenna to allow for measurement of the input impedance and radiation characteristics. The return loss for both the three- and five-silver-layer patch antennas is measured on an Anritzu 37369A and displayed in Fig. 3 along with the simulation of the three-silver-layer patch.

It can be seen that the three-layer patch is matched well with the simulation and is well matched to 50 Ω at 24.4 GHz. The five-layer patch is well matched at a lower frequency of 24.2 GHz, which is caused by increased ink spreading due to

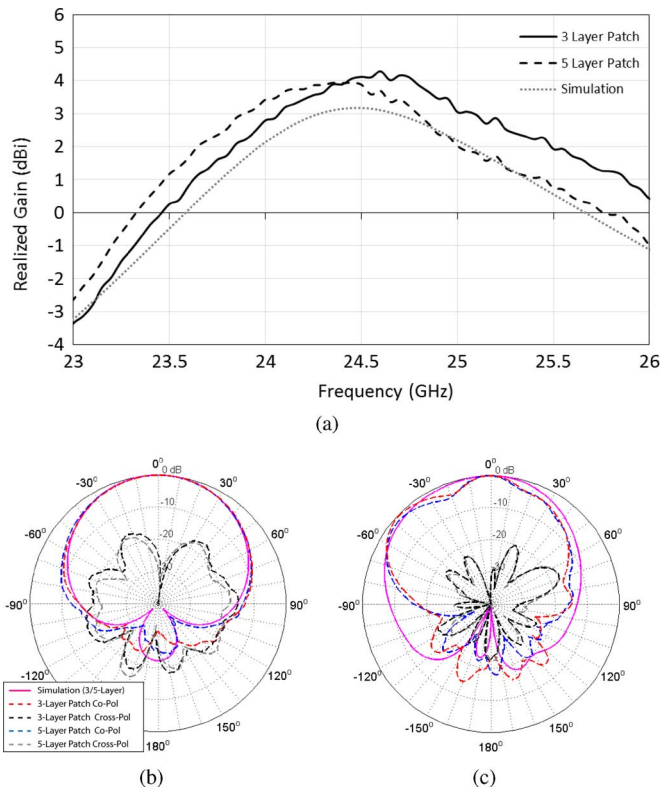


Fig. 4. (a) Simulated and measured broadside realized gain versus frequency of the coupled patch antenna, (b) simulated and measured normalized H-plane radiation pattern, and (c) simulated and measured normalized E-plane radiation pattern at 24.5 GHz.

the higher volume of dispensed ink. The return loss results show that even between fabrication batches, the inkjet process produces very repeatable results within 1%.

To measure the radiation pattern and gain, a far-field chamber that is calibrated using SA12A-18 standard gain horn antennas is utilized. The broadside realized gain values versus frequency of the three- and five-layer patch antennas are measured and compared to simulation in Fig. 4(a). The peak realized gain is approximately 4 dBi for both patch antennas. The results confirm that a conductor realized with three layers of silver is thick enough to account for skin depth above 24.5 GHz. The measured and simulated radiation patterns displayed in Fig. 4(c) and (d) are in good agreement. The slight discrepancies between measurement and simulation in the E-plane radiation pattern cut are due to the connector and feeding cables, which are positioned  $-90^\circ$ , not being included in the simulation to minimize computational time. The results of the proximity coupled patch confirm that inkjet printing is a viable and repeatable technology for processing mm-wave passive structures on-wafer and on-package that can potentially simplify the packaging process in a drastic way.

#### IV. PROXIMITY-FED PATCHARRAY DESIGN AND MEASUREMENTS

To demonstrate the reliability of the multilayer printing process, it is used print to a more complex four-element proximity-fed patch array for the 24.5-GHz band. The proximity

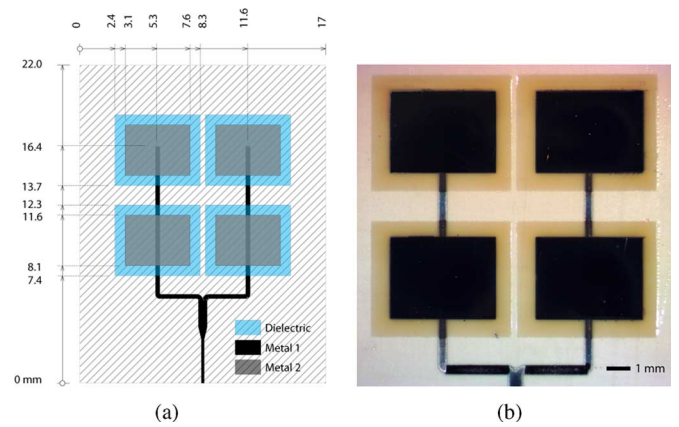


Fig. 5. (a) Design of the multilayer coupled patch antenna array. (b) Optical micrograph of the fabricated coupled patch antenna array on LCP substrate.

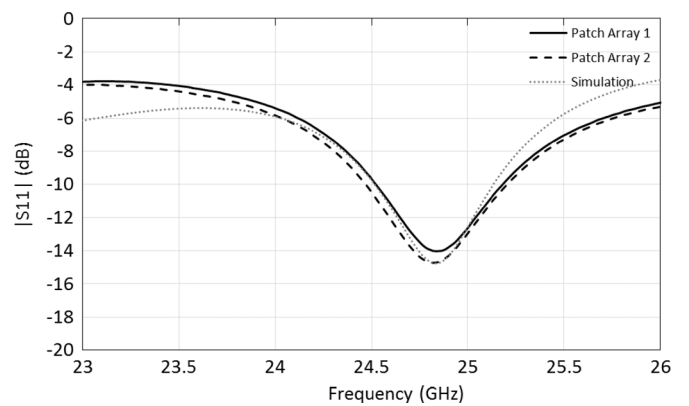


Fig. 6. Simulated and measured return loss of the coupled patch antenna array.

coupled array shown in Fig. 5(a) is an arrayed version of the proximity-fed patch in Section III. The patch array dimensions are optimized in the CST frequency domain solver for a  $50\text{-}\Omega$  input impedance and maximum broadside gain at 24.5 GHz.

The layer thicknesses are  $1.5\text{ }\mu\text{m}$  for the printed metal layers and  $60\text{ }\mu\text{m}$  for the printed SU-8 spacer. A thicker SU-8 layer is used to demonstrate the ease and versatility of changing layer thicknesses on-the-fly with inkjet printing, which in this case only requires two extra passes of the printer. The optimized simulation results yield a center-to-center element spacing of  $0.51\lambda$  in the horizontal direction and  $0.6\lambda$  in the vertical direction, and a patch size of  $3.5 \times 4.4\text{ mm}^2$ . The patch size is slightly larger than that of the single-element patch due to the thicker printed dielectric and mutual coupling between the elements. The fabrication is carried out following the previously outlined method in Section III, and an optical micrograph of a fabricated array is shown in Fig. 5(b). The post-fabrication measurements show the printed dielectric spacer to be  $64\text{ }\mu\text{m}$  thick, which is  $4\text{ }\mu\text{m}$  thicker than the initial specification, and the patch size to be  $3.52 \times 4.5\text{ mm}^2$ , which is very close to the specified dimensions in the layout. Return-loss measurements are performed on two arrays from the batch and compared to the post-fabrication simulation in Fig. 6. While the array is a much more complex structure to fabricate, it can be seen that the return loss between fabricated arrays is nearly identical and well matched to  $50\text{ }\Omega$  at 24.75 GHz. The frequency at which the antenna is well matched

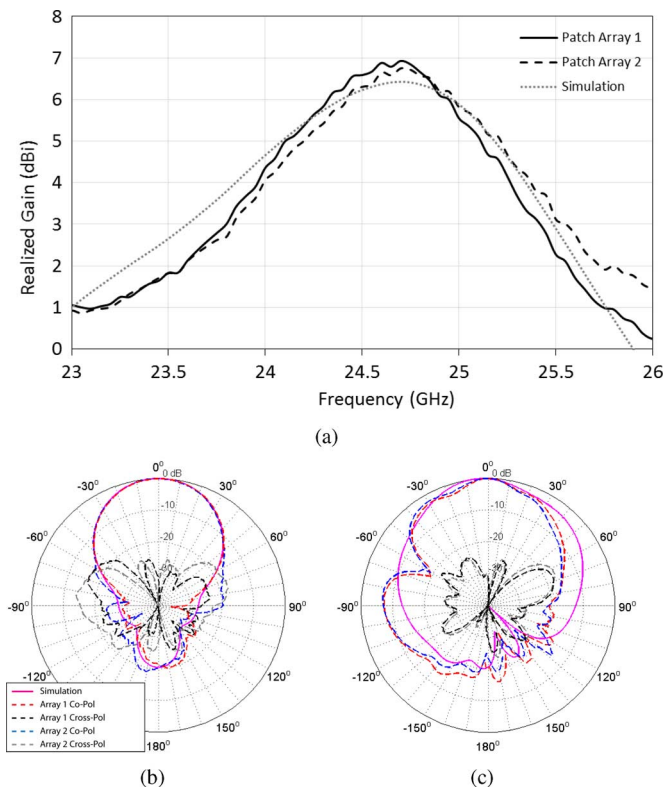


Fig. 7. (a) Simulated and measured broadside realized gain versus frequency of the coupled patch antenna. (b) Simulated and measured normalized H-plane radiation pattern. (c) Simulated and measured normalized E-plane radiation pattern.

is higher than the initial simulation due to small fabrication variations, but matches well with post-fabrication simulations. Following the return-loss measurements, the realized gain versus frequency and radiation patterns of the two arrays are measured and compared to simulation. In Fig. 7, it is shown that both arrays have a very similar broadside gain versus frequency with peak gains of 7 dBi. The measured E- and H-plane radiation pattern cuts shown in Fig. 7(c) and (b) respectively show a strong agreement between both fabricated arrays and the simulation. Again, there is a slight disagreement between measurement and simulation in the E-plane cut due to the lack of connector and cable radiation in the simulation.

## V. CONCLUSION

Utilizing inkjet printing in a novel layer-by-layer deposition approach, high-gain mm-wave antennas and antenna arrays that conventionally required complex fabrication methods and multilayer boards are rapidly and cheaply fabricated onto virtually any substrate with gains as high as 7 dBi. The resulting repeatability within 1% of the printing process shows a great promise in paving the road to on-package and on-chip printed antennas for inter/intrachip communications to greatly simplify the currently

complex antenna-on-package and chip-scale package-based design and fabrication techniques. While operation frequencies of 24.5 GHz are demonstrated in this letter for the first time for multilayer antennas topologies of enhanced complexity, the results show the potential of inkjet printing for printing structures at even higher frequencies. Future work in adding layers to the process stack-up and optimizing printed materials for higher frequencies will greatly enhance design and manufacturing capabilities and allow for smaller, cheaper, and conformally integrated mm-wave and subterahertz wireless systems.

## REFERENCES

- [1] B. S. Cook and A. Shamim, "Inkjet printing of novel wideband and high gain antennas on low-cost paper substrate," *IEEE Trans. Antennas Propag.*, vol. 60, no. 9, pp. 4148–4156, Sep. 2012.
- [2] B. S. Cook, J. R. Cooper, and M. M. Tentzeris, "Multi-layer, RF capacitors on flexible substrates utilizing inkjet printed dielectric polymers," *IEEE Microw. Wireless Compon. Lett.*, vol. 23, no. 7, pp. 353–355, Jul. 2013.
- [3] S. H. Ko, J. Chung, H. Pan, C. P. Grigoropoulos, and D. Poulidakos, "Fabrication of multilayer passive and active electric components on polymer using inkjet printing and low temperature laser processing," *Sensors Actuators*, vol. 134, pp. 161–168, 2007.
- [4] V. Subramanian, P. C. Chang, J. B. Lee, S. E. Molesa, and S. K. Volkman, "Printed organic transistors for ultra-low-cost RFID applications," *IEEE Trans. Compon. Packag. Technol.*, vol. 28, no. 4, pp. 742–747, Dec. 2005.
- [5] L. Yang, A. Rida, and M. M. Tentzeris, "Design and development of radio frequency identification (RFID) and RFID-enabled sensors on flexible low cost substrates," *Synth. Lect. RF/Microw.*, vol. 1, pp. 1–89, 2009.
- [6] L. Yang, A. Rida, R. Vyas, and M. M. Tentzeris, "RFID tag and RF structures on a paper substrate using inkjet-printing technology," *IEEE Trans. Microw. Theory Tech.*, vol. 55, no. 12, pp. 2894–2901, Dec. 2007.
- [7] S. Seok, N. Rolland, and P.-A. Rolland, "Millimeter-wave quarter-wave patch antenna on benzocyclobutene polymer," in *Proc. 38th Eur. Microw. Conf.*, 2008, pp. 1018–1021.
- [8] S. Hage-Ali, N. Tiercelin, P. Coquet, R. Sauleau, H. Fujita, V. Preobrazhensky, and P. Pernod, "A millimeter-wave microstrip antenna array on ultra-flexible micromachined polydimethylsiloxane (PDMS) polymer," *IEEE Antennas Wireless Propag. Lett.*, vol. 8, pp. 1306–1309, 2009.
- [9] G. DeJean, R. Bairavasubramanian, D. Thompson, G. E. Ponchak, M. M. Tentzeris, and J. Papapolymerou, "Liquid crystal polymer (LCP): A new organic material for the development of multilayer dual-frequency/dual-polarization flexible antenna arrays," *IEEE Antennas Wireless Propag. Lett.*, vol. 4, pp. 22–26, 2005.
- [10] B. J. Kang, C. K. Lee, and J. H. Oh, "All-inkjet-printed electrical components and circuit fabrication on a plastic substrate," *Micro-Nano-Eng.*, vol. 97, pp. 251–254, 2012.
- [11] D. Thompson, O. Tantot, H. Jallageas, G. Ponchak, M. Tentzeris, and J. Papapolymerou, "Characterization of liquid crystal polymer (LCP) material and transmission lines on LCP substrates from 30 to 110 GHz," *IEEE Trans. Microw. Theory Tech.*, vol. 52, no. 4, pp. 1343–1352, Apr. 2004.
- [12] A. Ghannam, C. Viallon, D. Bourrier, and T. Parra, "Dielectric microwave characterization of the SU-8 thick resin used in an above IC process," in *Proc. 39th Eur. Microw. Conf.*, 2009, pp. 1041–1044.
- [13] S. Vajha and S. Prasad, "Design and modeling of proximity coupled patch antenna," in *Proc. IEEE-APS Conf. Antennas Propag. Wireless Commun.*, 2000, pp. 43–46.
- [14] *Modern Antenna Handbook*, C. Balanis, Ed. Hoboken, NJ, USA: Wiley, 2008.